ACS Macro Letters

Letter

pubs.acs.org/macroletters

Light-Healable Supramolecular Nanocomposites Based on Modified Cellulose Nanocrystals

Mahesh V. Biyani, E. Johan Foster,* and Christoph Weder*

Adolphe Merkle Institute, Polymer Chemistry and Materials, University of Fribourg, Rte de l'Ancienne Papeterie, CH-1723 Marly 1, Switzerland

Supporting Information

ABSTRACT: Polymers that can be repaired after being damaged are attractive, because this feature can improve the reliability, functionality, and lifetime of these materials. We report here light-healable nanocomposites based on a telechelic poly(ethylene-*co*-butylene) that was functionalized with hydrogen-bonding ureidopyrimidone (UPy) and cellulose nanocrystals (CNCs) decorated with the same binding motif. These nanocomposites show significantly improved mechanical properties when compared to the supramolecular polymer alone. When these materials are exposed to ultraviolet radiation, the UPy motifs are excited and the absorbed energy is converted into heat. This causes temporary disengagement of the hydrogen-bonding motifs, concomitant with a reversible decrease of the supramolecular polymers' molecular weight and viscosity. As a result, deliberately introduced defects can be healed quickly and efficiently, even at a filler content of 20% w/w, that is, in compositions that exhibit high strength and stiffness.

Polymers that are repairable after being damaged are attractive for many applications because this feature can improve the reliability, functionality, and lifetime of a broad range of products.[1−8] Several routes are being explored to create such materials, including the use of supramolecular polymers that are assembled on the basis of noncovalent binding motifs.[9−12] This design allows one to temporarily reduce the molecular weight of the macromolecules by shifting the equilibrium to the monomer side by exposure to an appropriate stimulus. The resulting increase of the chain mobility and decrease of the material's viscosity enable the polymer to flow and fill cracks and gaps, before the original material is reformed by shifting the equilibrium back to the polymer side. We recently reported metallosupramolecular polymers based on this design, in which defects can be healed upon exposure to light.[13] These materials consist of a telechelic poly(ethylene-*co*-butylene) that was chain-terminated with 2,6-bis(1′-methylbenzimidazolyl)-pyridine ligands and assembled into polymeric structures with stoichiometric amounts of Zn^{2+} or La^{3+} salts. Upon exposure to ultraviolet radiation, the metal−ligand motifs are electronically excited and relax to the ground state in a nonradiative manner so that the absorbed energy is converted into heat. This facilitates the temporary dissociation of the metal−ligand motifs and transforms the material into a low-viscosity liquid, which can easily fill small defects. When the light is switched off, the metallopolymers reassemble and their original properties are restored. One attractive feature of healing with light is that the stimulus can be applied locally, that is, to only a portion of an object, so that objects can be healed under load.[13]

We here report how this design approach can be extended to create light-healable supramolecular nanocomposites, which offer much better mechanical properties than the supramolecular matrix alone. A telechelic poly(ethylene-*co*-butylene) functionalized with hydrogen-bonding ureidopyrimidone (UPy; Figure 1), groups at the termini, as first described by Sijbesma

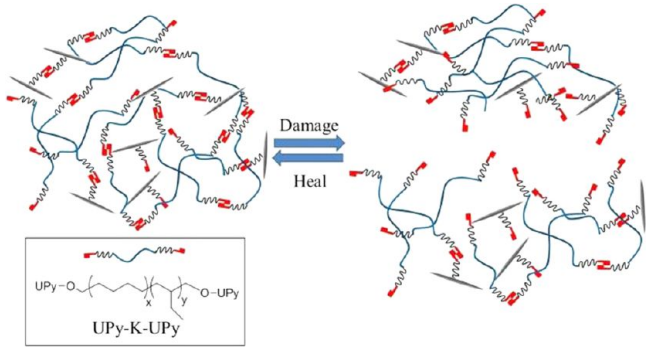

Figure 1. Schematic representation of the formation of a supramolecular nanocomposite based on UPy-K-UPy and UPy-decorated CNCs (CNC-UPy, cf. Scheme 1).

and Meijer,[14] was used as a supramolecular polymer matrix. This tacky, rubbery material with a storage modulus of 5−10 MPa has been shown to heal autonomously when freshly cut pieces were pressed together.[12] Cellulose nanocrystals (CNCs) were used as a nanofiller (Figure 2a). These bioderived nanofibers have dimensions of ≈5−30 × 100−2200 nm and exhibit a high on-axis modulus of ≈105−140 GPa, depending on the source.[15−17] CNCs are widely studied as fillers in

Received: February 7, 2013
Accepted: February 19, 2013
Published: February 27, 2013

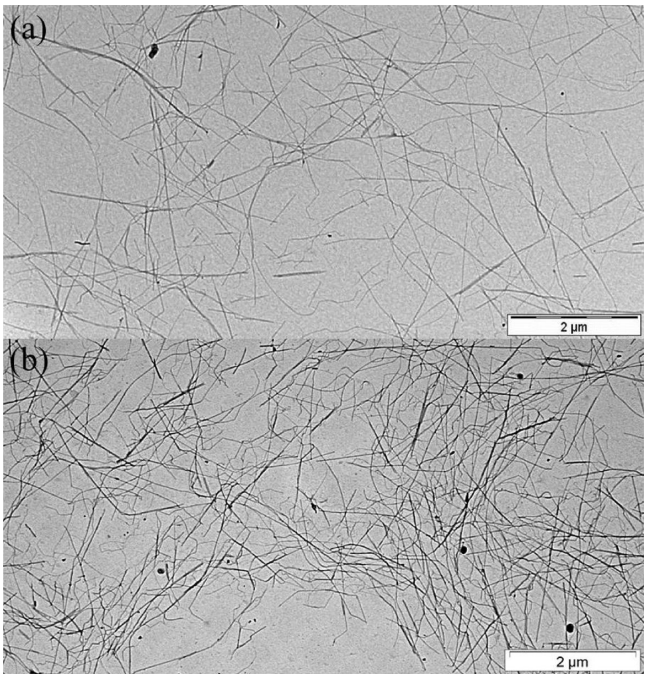

Figure 2. Transmission electron micrographs of (a) unmodified CNCs and (b) CNC-UPy. Samples were prepared by drop-casting 0.1 mg/mL DMF dispersions on carbon-coated copper grids.

polymer nanocomposites,[18−22] including mechanically adaptive materials where the CNC−CNC and CNC−matrix interactions can be controlled by an external stimulus.[3,23−27] Unmodified CNCs were recently employed to reinforce a thermally healable supramolecular polymer formed via $\pi-\pi$ interactions between a π-electron rich pyrenyl end-capped oligomer and a chain-folding oligomer containing pairs of π-electron poor naphthalene-diimide units.[28] In the case of the present light-healable nanocomposites, the use of unmodified CNCs is not effective (vide infra) and UPy-derivatized CNCs were used instead (Figure 1, Scheme 1). This design roots in the hypothesis that

Scheme 1. Decoration of Cellulose Nanocrystals (CNCs) with 2-(6-Isocyanatohexylaminocarbonyl amino)-6-methyl-4[1*H*]pyrimidinone (UPy-NCO)

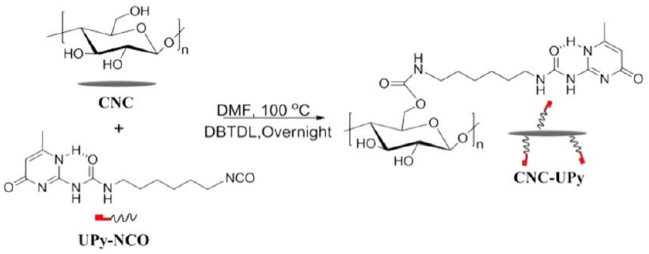

specific, optically addressable, CNC−CNC and CNC−matrix interactions could improve the homogeneity of the system and impart efficient healing behavior.

Non-surface-modified CNCs were isolated by sulfuric acid hydrolysis from the mantles of tunicates using an established protocol (see Supporting Information, SI, for experimental details).[24,25] They had an average length of 1720 ± 514 nm, a width of 25 ± 6 nm, an aspect ratio of 69 (Figure 2a), and a surface charge density of about 75 mmol/kg, which is related to sulfate ester surface groups introduced during hydrolysis with H_2SO_4 (Figure S1 in SI). The CNCs were decorated with UPy groups by reacting a CNC dispersion in DMF with a stoichiometric amount (relative to all OH groups in the CNCs) of 2-(6-isocyanatohexylaminocarbonylamino)-6-methyl-4[1*H*]pyrimidinone (UPy-NCO, Scheme 1)[14] at 100 °C, using a catalytic amount of dibutyltindilaurate. The modified CNCs were separated from the reaction mixture by centrifugation, washed with DMF, and kept dispersed in DMF, as the modified CNCs (referred to as CNC-UPy) did not redisperse well after lyophilization. Reaction yield, IR spectra (Figure S2 in SI), elemental analysis (Table S1 in SI), and UV−vis absorption spectra (Figure S3 in SI) confirm the success of the reaction and reveal that the CNC-UPy sample contains ≈12% w/w of UPy-NCO residue. This corresponds to a degree of substitution of 0.18, which corresponds to essentially full conversion of the available surface OH groups.[29−32] The resulting CNC-UPy form a stable dispersion in DMF, remain well-separated when dried (Figure 2b), and their average length (1770 ± 560 nm), width (26 ± 6 nm), and aspect ratio (68) are identical to those of the original CNCs.

Nanocomposite films composed of UPy-K-UPy and 10% w/w unmodified CNCs or 10, 15, or 20% w/w CNC-UPy (the latter comprising 12% w/w of UPy-NCO residue and 88% w/w of cellulose) were prepared by solution-casting from THF, which was identified as the best common solvent for UPy-K-UPy and CNC-UPy. After drying, the nanocomposites were reshaped by compression molding (Figure S4 in SI) and the resulting films had a thickness of 200−250 μm. The films made from UPy-K-UPy and 10% w/w unmodified CNCs displayed macroscopic phase separation (Figure S4b in SI). As a consequence, the mechanical properties varied widely between different samples (Figure S5 and Table S2 in SI). The observed phase separation might in part be related to the fact that THF is not a very good dispersant for unmodified CNCs,[33] but the more homogeneous nature of other THF-based nanocomposites with unmodified CNCs suggests that unmodified CNCs and UPy-K-UPy are poorly miscible.[33] By contrast, the combination of CNC-UPy and UPy-K-UPy led to the formation of transparent nanocomposite films with homogeneous appearance (Figure S4b in SI). Their mechanical properties were established by dynamic mechanical analysis (DMA) and tensile testing (Table 1). The tensile storage moduli (E'), measured by DMA as a function of temperature, are shown in Figure 3a. At −60 °C, the neat UPy-K-UPy matrix is in a glassy state and displays an E' of about 1.2 GPa; E' is drastically reduced when the temperature is increased above the glass transition temperature (T_g, ca. −50 °C), and a broad rubbery plateau is seen between about 0 and 60 °C. Above the latter temperature, phase-separated UPy stacks, which serve as physical cross-links, melt and the material fails.[14] The incorporation of CNC-UPy led to a modest stiffness increase below T_g, where E' increased from 1.2 GPa for the neat UPy-K-UPy to 3.0 GPa for the nanocomposite comprising 20% w/w CNC-UPy. A much more pronounced reinforcement is seen in the rubbery regime (e.g., at 20 °C), where E' increased from 10 MPa for the neat UPy-K-UPy to 247 MPa for the nanocomposite comprising 20% w/w CNC-UPy.

The data extracted from tensile tests (Figure 3b) paint a similar picture as the DMA data. The Young's modulus changed in a similar manner as E' (Table 1), the maximum stress increased from 1.6 (neat UPy-K-UPy) to 4.4 MPa (20% w/w CNC-UPy), while the strain to break was considerably

dx.doi.org/10.1021/mz400059w | *ACS Macro Lett.* 2013, 2, 236−240

Table 1. Mechanical Properties of Neat UPy-K-UPy and UPy-K-UPy/CNC-UPy Nanocomposites

samples	Young's modulus (MPa)[a]	maximum stress (MPa)[a]	strain at break (%)[a]	storage modulus (MPa)[b]
UPy-K-UPy				
original	13 ± 4	1.6 ± 0.1	51.5 ± 3.6	10 ± 3
damaged		1.1 ± 0.1	19.2 ± 0.4	
optically healed (350 mW/cm^2, 20 s)	13 ± 2	1.2 ± 0.2	26.5 ± 3.1	
optically healed (350 mW/cm^2, 80 s)	16 ± 4	1.3 ± 0.1	37.4 ± 8.4	
UPy-K-UPy/CNC-UPy 10% w/w				
original	62 ± 5	2.3 ± 0.7	18.9 ± 0.9	59 ± 17
damaged		1.1 ± 0.1	3.7 ± 0.2	
optically healed (350 mW/cm^2, 20 s)	56 ± 4	1.8 ± 0.1	15.1 ± 2.7	
optically healed (250 mW/cm^2, 80 s)	50 ± 4	1.9 ± 0.1	12.3 ± 2.3	
UPy-K-UPy/CNC-UPy 15% w/w				
original	103 ± 6	3.6 ± 0.1	8.2 ± 0.5	126 ± 27
damaged		2.2 ± 0.7	3.7 ± 0.7	
optically healed (350 mW/cm^2, 20 s)	89 ± 6	2.3 ± 0.4	6.6 ± 2.4	
optically healed (250 mW/cm^2, 80 s)	104 ± 12	3.7 ± 0.2	7.9 ± 0.2	
UPy-K-UPy/CNC-UPy 20% w/w				
original	158 ± 25	4.4 ± 0.5	6.0 ± 1.0	247 ± 30
damaged		2.9 ± 0.4	2.3 ± 0.3	
optically healed (350 mW/cm^2, 20 s)	110 ± 10	3.0 ± 0.1	9.9 ± 1.3	
optically healed (250 mW/cm^2, 80 s)	170 ± 20	4.5 ± 0.6	3.9 ± 0.3	

[a]Measured by stress−strain experiments. [b]Measured by DMA. Samples were optically healed by exposure to light of a wavelength of 320−390 nm. Averages represent data from three independently made compositions, from which at least three samples per film were measured. All stress−strain tests were conducted at 25 °C.

reduced from about 51 (neat polymer) to 6% (20% w/w CNC-UPy).

The UPy motif displays an absorbance band centered around 282 nm (Figure S3 in SI), which, due to the low concentration of the binding motif, is however hardly distinguishable in films on the neat UPy-K-UPy (Figure S6 in SI). By contrast, the UPy absorption is clearly seen in the UPy-K-UPy/CNC-UPy nanocomposites (Figure S6 in SI) in which the local UPy concentration is much higher and subsequent stacking of the UPy causes an increase in the absorption centered around 282 nm.[34] In fact, the absorbance at 290 nm of 40 or 60 μm thick films with 15 or 10% w/w CNC-UPy is about 2.5, which allows essentially quantitative absorption of incident light. The optical healing approach pursued here is based on the hypothesis that the optically absorbed energy is converted into heat, so that the supramolecular nanocomposites dissociate, liquefy, and allow defects to heal.

To probe this, films of the nanocomposites were damaged by applying well-defined cuts with a depth of about 50−70% of their thickness (Figure S7 in SI). These samples were subsequently exposed to UV irradiation with a wavelength of 320−390 nm with an intensity of 250−350 mW/cm^2 (SI, Movie S1). It is noted that the light source was chosen based on availability and not optimally matched with the UPy absorption spectrum. Optical inspection of the samples composed of the neat UPy-K-UPy reveals that at an intensity of 350 mW/cm^2 an exposure of 80 s is required to heal the cut. Due to the higher optical density, the nanocomposite samples containing 10% w/w of CNC-UPy were found to heal considerably faster, requiring less than 20 s of UV exposure (Figure 4a). AFM images taken before, during, and after healing confirm that also on the nanoscale, the original topology is indeed restored (Figure 4b and S8 in SI). Damaged samples of nanocomposites containing 15 or 20% w/w of CNC-UPy began to smoke when irradiated under the same conditions (350 mW/cm^2, 20 s), which is attributed to the higher optical absorption, causing excessive heating (Table S4 in SI) and thermal decomposition. When these samples were exposed to light of lower intensity and longer time (250 mW/cm^2, 80 s), they were visually found to heal as effectively as the 10% UPy-K-UPy/CNC-UPy nanocomposites.

To quantitatively determine the healing efficiency of the new nanocomposites, films of the various compositions were damaged and healed as described above and the mechanical properties of original, damaged, and healed samples were elucidated by stress−strain experiments (Table 1, Figure 3b). Reference experiments in which the samples were thermally healed by heating them in an oven at 70 °C for 10 min in case of the neat UPy-K-UPy and 20 min in case of the nanocomposites of UPy-K-UPy and 10 or 15% w/w CNC-UPy were also conducted (Figure S8, Table S3 in SI). Figure 3b shows that the maximum stress and strain at break of a film of the neat UPy-K-UPy are significantly reduced when the sample was damaged by a cut as described above. While exposure to heat led to complete healing, irradiation with UV light caused only partial restoration of the original properties, consistent with the low optical absorption of this material. In case of the nanocomposite containing 10% w/w of CNC-UPy, the optical healing is rather efficient. The data shown in Table 1 reveal that the healed sample is slightly weaker than the original, but the difference is barely statistically significant. Gratifyingly, the mechanical properties could be fully restored in nanocomposites containing 15 or 20% w/w CNC-UPy, but only when irradiated at lower intensity and longer time (250 mW/cm^2, 80 s, Table 1, Figure 3b). Thus, even nanocomposites with a rather high CNC-UPy concentration, in which the mechanical

dx.doi.org/10.1021/mz400059w | ACS Macro Lett. 2013, 2, 236−240

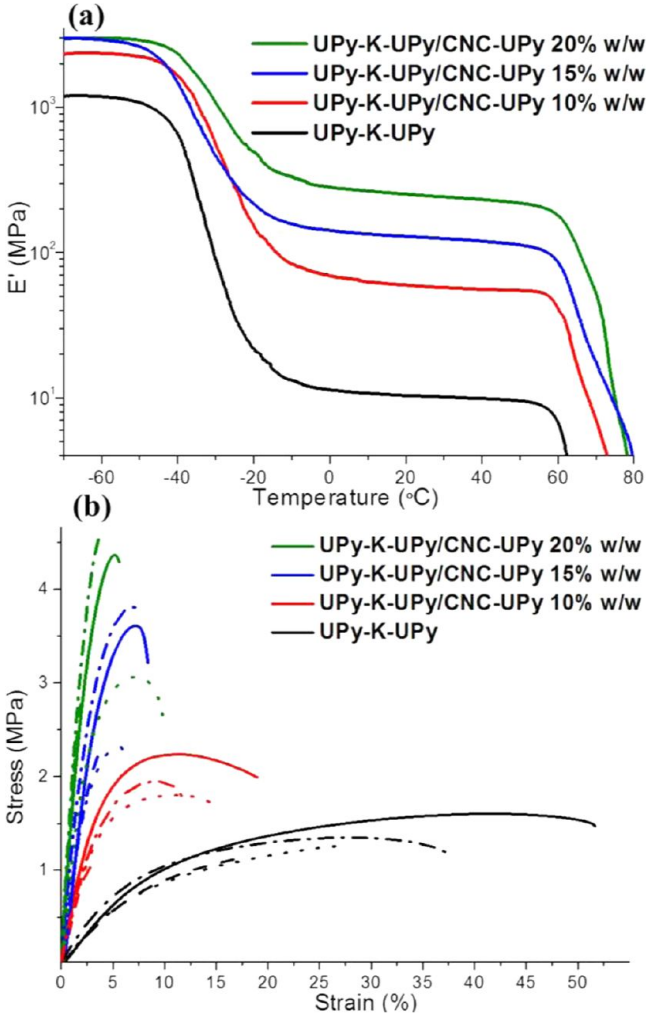

Figure 3. (a) DMA traces of films of UPy-K-UPy and nanocomposites of UPy-K-UPy and 10, 15, or 20% w/w CNC-UPy. (b) Stress–strain curves of the same materials. Solid lines = original samples; dashed lines = deliberately damaged samples; dotted lines = optically healed samples with a power density of 350 mW/cm^2 for 20 s; and dash-dotted lines = optically healed samples with a power density of 250 mW/cm^2 for 80 s.

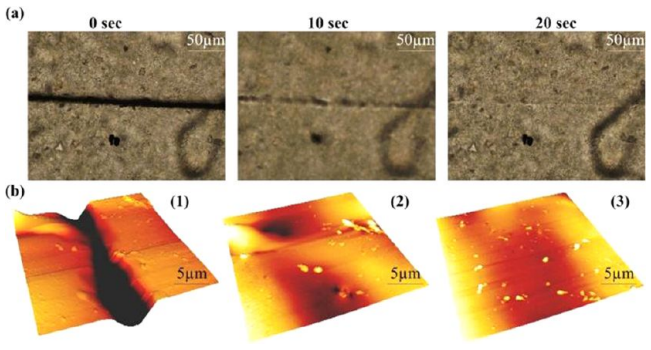

Figure 4. (a) Optical microscope images of deliberately damaged UPy-K-UPy/CNC-UPy 10% w/w nanocomposite films before, during, and after exposure to UV light (320–390 nm, 350 mW/cm^2, 20 s). (b) Atomic force micrographs of UPy-K-UPy/CNC-UPy 10% w/w nanocomposite films in the deliberately damaged (1), partially healed (2), and completely healed (3) state (color range; black = 7 μm, white = 0 μm).

reinforcement is very significant, exhibit very efficient and rapid optical healing. This finding is in contrast to the behavior seen in the few known examples in which healable polymers were reinforced with unmodified CNCs (i.e., the reference material reported herein, the metallosupramolecular polymers investigated by us, and the supramolecular polymer formed via π–π interactions reported by Rowan and co-workers[28]), where healability was compromised at CNC concentrations of more than about 10%. One may speculate that this limitation stems from the significant attractive interactions between unmodified CNCs on account of hydrogen bonding via their surface hydroxyl groups, which is likely to stifle dissociation of the CNC network and efficient rearrangement of the CNCs during healing process. The data presented here suggest that the introduction of surface groups that display specific reversible interactions among the CNCs and between the CNCs and the supramolecular matrix helps to remedy this problem.

In conclusion, we have shown that supramolecular nanocomposites composed of a hydrogen-bonded supramolecular polymer and cellulose nanocrystals decorated with the same supramolecular motif display an intriguing combination of high stiffness, high strength, and rapid and efficient optical healing. These properties appear to be the result of the specific design, which leads to full integration of filler and matrix to the extent where these components can no longer be distinguished and permits the temporary disengagement of *all* relevant supramolecular interactions during the healing process. This approach was exploited here to create optically healable supramolecular nanocomposites based on the hydrogen-bonding UPy motif, but it appears that the framework can be adapted to other binding motifs, stimuli, and fillers.

■ ASSOCIATED CONTENT

Ⓢ Supporting Information

Experimental section detailing the methods employed, the isolation of CNCs from tunicates and their functionalization with UPy groups, the synthesis of telechelic poly(ethylene-*co*-butylene) with terminal UPy groups, the preparation and characterization of the nanocomposites, along with UV–vis and FT-IR spectra and DMA data not presented in the paper (Tables S1–S4 and Figures S1–S9), and a movie showing an optical healing experiment (Movie S1). Also available is additional detail presented in a movie. This material is available free of charge via the Internet at http://pubs.acs.org.

■ AUTHOR INFORMATION

Corresponding Author

*E-mail: johan.foster@unifr.ch; christoph.weder@unifr.ch.

Notes

The authors declare no competing financial interest.

■ ACKNOWLEDGMENTS

The authors gratefully acknowledge financial support from the Swiss National Science Foundation (NRP 62: Smart Materials, Nr. 406240_126046) and the Adolphe Merkle Foundation. Authors would also like to acknowledge Dr. Gina Fiore and Souleymane Coulibaly for assistance with the optical healing experiments and Sandra Camarero Espinosa for conducting the AFM study.

■ REFERENCES

(1) Bergman, S. D.; Wudl, F. *J. Mater. Chem.* **2008**, *18*, 41.

(2) Burattini, S.; Greenland, B. W.; Chappell, D.; Colquhoun, H. M.; Hayes, W. *Chem. Soc. Rev.* **2010**, *39*, 1973.
(3) Murphy, E. B.; Wudl, F. *Prog. Polym. Sci.* **2010**, *35*, 223.
(4) Syrett, J. A.; Becer, C. R.; Haddleton, D. M. *Polym. Chem.* **2010**, *1*, 978.
(5) Guimard, N. K.; Oehlenschlaeger, K. K.; Zhou, J.; Hilf, S.; Schmidt, F. G.; Barner-Kowollik, C. *Macromol. Chem. Phys.* **2012**, *213*, 131.
(6) Zhang, H.; Xia, H.; Zhao, Y. *ACS Macro Lett.* **2012**, *1*, 1233.
(7) Imbesi, P. M.; Fidge, C.; Raymond, J. E.; Cauët, S. I.; Wooley, K. L. *ACS Macro Lett.* **2012**, *1*, 473.
(8) Luo, X.; Mather, P. T. *ACS Macro Lett.* **2013**, 152.
(9) Bosman, A. W.; Sijbesma, R. P.; Meijer, E. W. *Mater. Today* **2004**, *7*, 34.
(10) Cordier, P.; Tournilhac, F.; Soulie-Ziakovic, C.; Leibler, L. *Nature* **2008**, *451*, 977.
(11) Chen, Y.; Kushner, A. M.; Williams, G. A.; Guan, Z. *Nat. Chem.* **2012**, *4*, 467.
(12) van Gemert, G. M. L.; Peeters, J. W.; Söntjens, S. H. M.; Janssen, H. M.; Bosman, A. W. *Macromol. Chem. Phys.* **2012**, *213*, 234.
(13) Burnworth, M.; Tang, L.; Kumpfer, J. R.; Duncan, A. J.; Beyer, F. L.; Fiore, G. L.; Rowan, S. J.; Weder, C. *Nature* **2011**, *472*, 334.
(14) Folmer, B. J. B.; Sijbesma, R. P.; Versteegen, R. M.; van der Rijt, J. A. J.; Meijer, E. W. *Adv. Mater.* **2000**, *12*, 874.
(15) Eichhorn, S. J. *ACS Macro Lett.* **2012**, *1*, 1237.
(16) Bras, J.; Viet, D.; Bruzzese, C.; Dufresne, A. *Carbohydr. Polym.* **2011**, *84*, 211.
(17) Šturcová, A.; Davies, G. R.; Eichhorn, S. J. *Biomacromolecules* **2005**, *6*, 1055.
(18) Azizi Samir, M. A. S.; Alloin, F.; Dufresne, A. *Biomacromolecules* **2005**, *6*, 612.
(19) Eichhorn, S. J.; Dufresne, A.; Aranguren, M.; Marcovich, N. E.; Capadona, J. R.; Rowan, S. J.; Weder, C.; Thielemans, W.; Roman, M.; Renneckar, S.; Gindl, W.; Veigel, S.; Keckes, J.; Yano, H.; Abe, K.; Nogi, M.; Nakagaito, A. N.; Mangalam, A.; Simonsen, J.; Benight, A. S.; Bismarck, A.; Berglund, L. A.; Peijs, T. *J. Mater. Sci.* **2010**, *45*, 1.
(20) Habibi, Y.; Lucia, L. A.; Rojas, O. J. *Chem. Rev.* **2010**, *110*, 3479.
(21) Klemm, D.; Kramer, F.; Moritz, S.; Lindström, T.; Ankerfors, M.; Gray, D.; Dorris, A. *Angew. Chem., Int. Ed.* **2011**, *50*, 5438.
(22) Tkalya, E.; Ghislandi, M.; Thielemans, W.; van der Schoot, P.; de With, G.; Koning, C. *ACS Macro Lett.* **2013**, 157.
(23) Capadona, J. R.; Shanmuganathan, K.; Tyler, D. J.; Rowan, S. J.; Weder, C. *Science* **2008**, *319*, 1370.
(24) Shanmuganathan, K.; Capadona, J. R.; Rowan, S. J.; Weder, C. *J. Mater. Chem.* **2010**, *20*, 180.
(25) Hsu, L.; Weder, C.; Rowan, S. J. *J. Mater. Chem.* **2011**, *21*, 2812.
(26) Mendez, J.; Annamalai, P. K.; Eichhorn, S. J.; Rusli, R.; Rowan, S. J.; Foster, E. J.; Weder, C. *Macromolecules* **2011**, *44*, 6827.
(27) Way, A. E.; Hsu, L.; Shanmuganathan, K.; Weder, C.; Rowan, S. J. *ACS Macro Lett.* **2012**, *1*, 1001.
(28) Fox, J.; Wie, J. J.; Greenland, B. W.; Burattini, S.; Hayes, W.; Colquhoun, H. M.; Mackay, M. E.; Rowan, S. J. *J. Am. Chem. Soc.* **2012**, *134*, 5362.
(29) Goussé, C.; Chanzy, H.; Excoffier, G.; Soubeyrand, L.; Fleury, E. *Polymer* **2002**, *43*, 2645.
(30) Braun, B.; Dorgan, J. R. *Biomacromolecules* **2009**, *10*, 334.
(31) Trejo-O'Reilly, J. A.; Cavaille, J. Y.; Gandini, A. *Cellulose* **1997**, *4*, 305.
(32) Siqueira, G.; Bras, J.; Dufresne, A. *Langmuir* **2010**, *26*, 402.
(33) Schroers, M.; Kokil, A.; Weder, C. *J. Appl. Polym. Sci.* **2004**, *93*, 2883.
(34) Brunsveld, L.; Vekemans, J.; Hirschberg, J.; Sijbesma, R. P.; Meijer, E. W. *Proc. Natl. Acad. Sci. U.S.A.* **2002**, *99*, 4977.